Case Studies in Nondestructive Testing and Evaluation 3 (2015) 9–14

Contents lists available at ScienceDirect

Case Studies in Nondestructive Testing and Evaluation

www.elsevier.com/locate/csndt

# Characterization of planar flaws by synthetic focusing of sound beam using linear arrays

Paritosh Nanekar [a,*], Anish Kumar [b], T. Jayakumar [b]

[a] *Bhabha Atomic Research Centre, Trombay, Mumbai - 400085, Maharashtra, India*
[b] *Indira Gandhi Centre for Atomic Research, Kalpakkam - 603102, Tamil Nadu, India*

ARTICLE INFO

*Article history:*
Available online 16 January 2015

ABSTRACT

Characterization of planar flaws by non-destructive evaluation is crucial from the point of view of structural integrity assessment. An approach involving SAFT processing of B-scan image collected by electronic scanning using linear array has been used for detection and characterization of planar flaws. The study was carried out on stainless steel plate with slots inclined at various orientations and carbon steel plates having implanted weld planar flaws. The results of these investigations are presented in this paper.


## 1. Introduction

Planar flaws are considered harmful from the point of view of structural integrity of the pressurized components because of the stress concentration associated with them. Manufacturing processes such as forging, rolling, welding, etc. can introduce planar flaws in the component. Service induced flaws such as fatigue cracks and stress corrosion cracks are also planar flaws. A crucial parameter determining the acceptability of a planar flaw is its depth (height or through-wall dimension) [1]. The amplitude based ultrasonic methods for flaw depth estimation are prone to errors primarily because of the fact that the signal amplitude from a flaw is dependent on many factors not related to flaw depth such as orientation, roughness, transparency and coupling efficiency [2]. Advanced ultrasonic based approaches reply on locating the flaw extremities and hence are less prone to sizing errors.

The time-of-flight diffraction technique uses a separate transmitter and receiver and relies on the time-of-flight of the diffracted signals from the flaw tips for depth sizing [3,4]. Synthetic Aperture Focusing Technique (SAFT) aims at locating the flaw tips and improving signal to noise ratio by carrying out post-processing of ultrasonic B-scan and C-scan images collected using a divergent sound beam [5,6]. During processing, the sound beams are time shifted or back propagated to the scattering source and averaged out using wave propagation formulae. The signal amplitude at the defect location is highly improved due to constructive interference, while at other locations the destructive interference of sound beam leads to huge drop in signal amplitude [7,8].

In the present study, an approach combining linear arrays and SAFT has been employed for characterization of planar flaws. The approach involves SAFT processing of B-scan image collected during electronic scanning using a linear array. The results of flaw characterization on a stainless steel plate with simulated planar flaws and carbon steel plates with weld planar flaws are discussed in this paper.

* Corresponding author. Tel.: +91 22 25594867.
*E-mail address:* pnanekar@barc.gov.in (P. Nanekar).

http://dx.doi.org/10.1016/j.csndt.2015.01.001

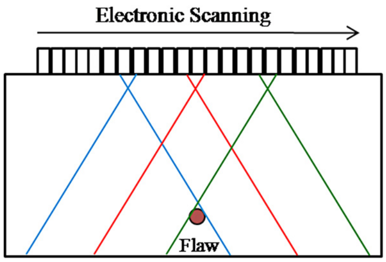


**Fig. 1.** Data acquisition using SFLA approach.

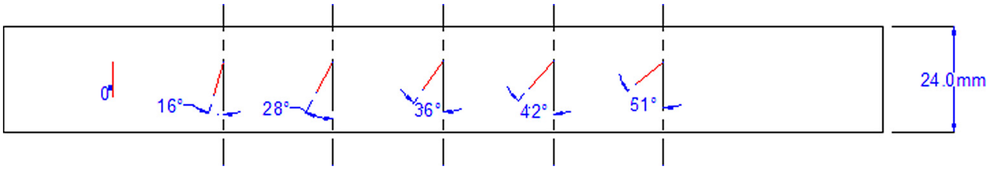


**Fig. 2.** Inclined slots in 24 mm thick stainless steel plate.

## 2. Array based ultrasonic methods for characterization of planar flaws

Linear arrays are increasingly being used for flaw detection and characterization in engineering components. Conventional phased array is based on the use of focal laws to steer and focus the sound beam [9,10]. Linear arrays with digital signal processing have also been reported for flaw characterization [11]. In Full Matrix Capture (FMC), the raw B-scan data is collected by using a single element as transmitter and all elements as receivers [12,13]. Once the data is acquired using FMC, the imaging of the target region is done using Total Focusing Method (TFM). With TFM, the region of interest is discretized into grids and the beam is focused at every point in the grid by summing up the signals from all the elements in an array. FMC approach leads to high resolution imaging for enhanced detection and sizing of flaws. However, the data size becomes large, especially while dealing with an array with large number of elements.

An approach combining a linear array with SAFT, named as SFLA, has been used in this study. This approach offers many advantages. Firstly, since smaller element size can easily be realized in a linear array transducer, one can achieve a good amount of beam divergence, which is crucial for SAFT processing. Secondly, the near field length is limited to a very short distance (less than a millimeter), thus ensuring that SAFT processing is effective for the full thickness of the sample. Thirdly, by using the electronic scanning approach of phased array, not only physical movement of the transducer is avoided, but it also ensures that the raw data is collected at much smaller increments corresponding to the element pitch. Another significant advantage is the huge reduction in the equipment cost as compared to the one required for conventional phased array. Since only one channel is used for data collection, a single channel multiplexed system, with a provision to connect large number of array elements can replace the costly and bulky conventional phased array instrument. Use of single element for transmission, may restrict the penetration of sound, especially in materials with high sound attenuation, which could be a limitation of this approach. Also, since the reception is by a single element and not by all, the signal-to-noise ratio is expected to be inferior to FMC.

Fig. 1 schematically depicts the methodology followed for imaging of flaws using the SFLA approach. A single element is used for transmission and reception. The raw B-scan image collected during electronic scan by a divergent sound beam is processed by time based SAFT algorithm.

## 3. Experimental details

Six slots oriented at angles ranging from 0° to 51°, having 8.5 mm length, 2 mm width and 25 mm depth, were machined by electro-discharge machining in 24 mm thick stainless steel plate from one of the faces, as shown in Fig. 2. These machine flaws represent fusion line defects in the weld joints or cracks in forged and rolled products in carbon steel or low alloy steel material. However, these inclined slots do not represent fusion-line defects in austenitic stainless steel welds, as the influence of inhomogeneous and anisotropic microstructure needs to be considered. Additionally, studies were carried out on carbon steel plates with embedded weld flaws (Fig. 3) in the form of (a) lack of fusion and (b) root crack. These are natural flaws and have been intentionally produced during welding. The samples had surface finish of better than 6 micron, which is stipulated in ASME Boiler and Pressure Vessel Code Section [14].

The ultrasonic data was collected using M2M make Multi 2000 Phased Array system having a configuration of 64 × 256. The data on the carbon steel weld samples was collected using a 10 MHz, 0.3 mm pitch, 128 elements linear array transducer. A 5 MHz, 0.6 mm pitch, 64 elements linear array was used for stainless steel plate. Specific software was developed in LabVIEW® for post-processing of the data using time-domain SAFT algorithm. To study the effectiveness of SFLA approach for flaw characterization, the flaws were also imaged by FMC + TFM approach using 64 parallel receivers.

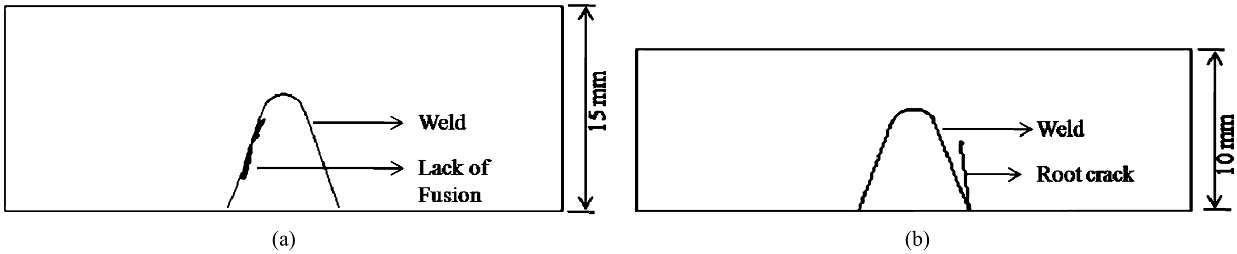


**Fig. 3.** Implanted planar weld flaws (a) lack-of fusion and (b) root crack.

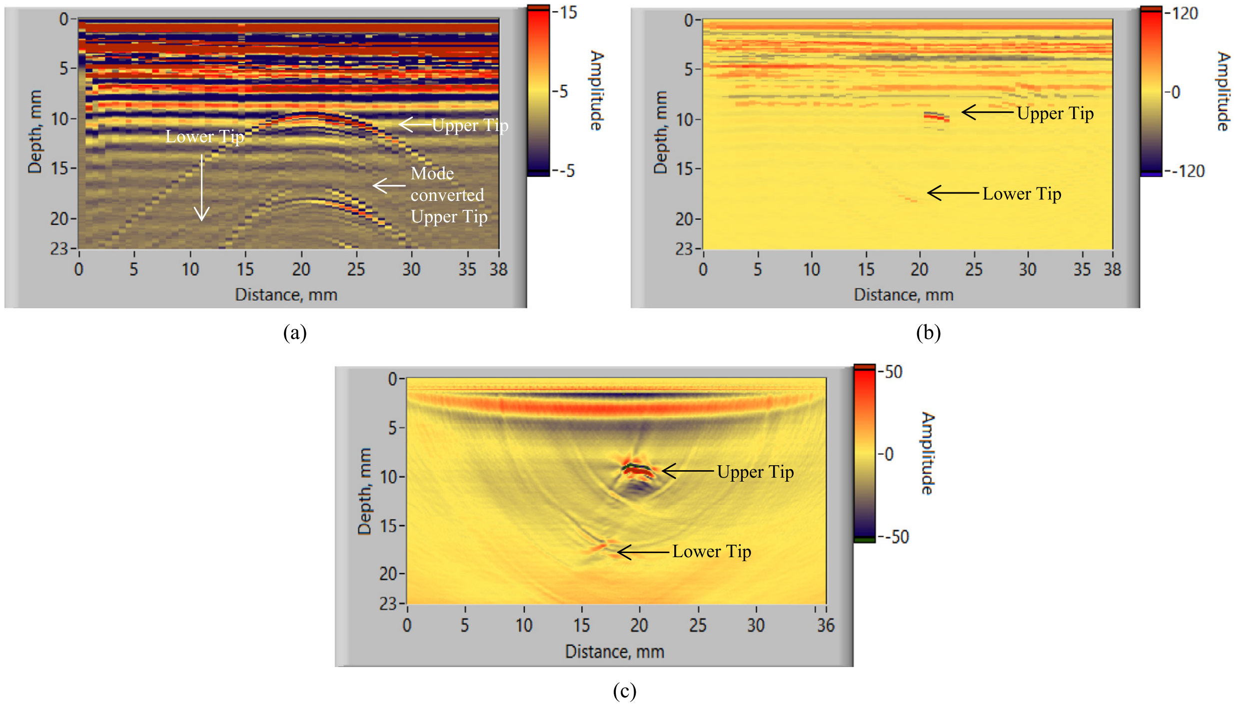


**Fig. 4.** B-scan image for a 16° oriented flaw (a) raw SFLA data, (b) processed SFLA data and (c) FMC + TFM data.

## 4. Results and discussions

### *4.1. Block 1: stainless steel plate with inclined slots*

Fig. 4a shows the raw B-scan image for a 16° inclined slot in the stainless steel plate using SFLA approach. From the image, one can see that the upper tip of the flaw shows a strong signal over a wide range as it is seen by the sound beam emanating from all the elements. Contrary to this, because of the flaw-tilt, the bottom tip signal is seen over a relatively narrow range, as it is seen only by the elements which lie on one side of the flaw. The image also shows a signal at approximately 1.5 times the time-of-flight of the signal corresponding to the upper flaw tip. This signal is from the mode converted shear wave, which is generated when the longitudinal wave is incident at the upper flaw tip. For the mode converted signal, the sound beam travels in the longitudinal mode (L) during the onward path and as a shear wave (S) during the return path. The velocity of shear wave is approximately half of that of the longitudinal wave in a material. Hence, the time-of-flight of this signal (LS) is approximately 1.5 times the time-of-flight of the signal (LL) that travels as longitudinal wave, both during onward and return path. The SAFT processed image is shown in Fig. 4b. During the SAFT processing, the mode converted signal gets eliminated due to the averaging, leaving behind only the LL signals from the upper and the lower tip of the flaws. From the SAFT processed image, one can accurately locate the flaw extremities and evaluate the height of the flaw. One can also find the orientation of the flaw with respect to the surface normal. Both these parameters are vital for fitness-for-service assessment. The result obtained by FMC + TFM approach for this flaw is shown in Fig. 4c.

Fig. 5 shows the raw, SFLA and FMC + TFM B-scan images for a flaw oriented at 51°. The processed images, in addition to the flaw tips, also show the flaw surface. When the divergent sound beam is incident on the flaw, a part of the reflected sound beam goes back to the receiving element since it is at near normal incidence to flaw surface. These signals are

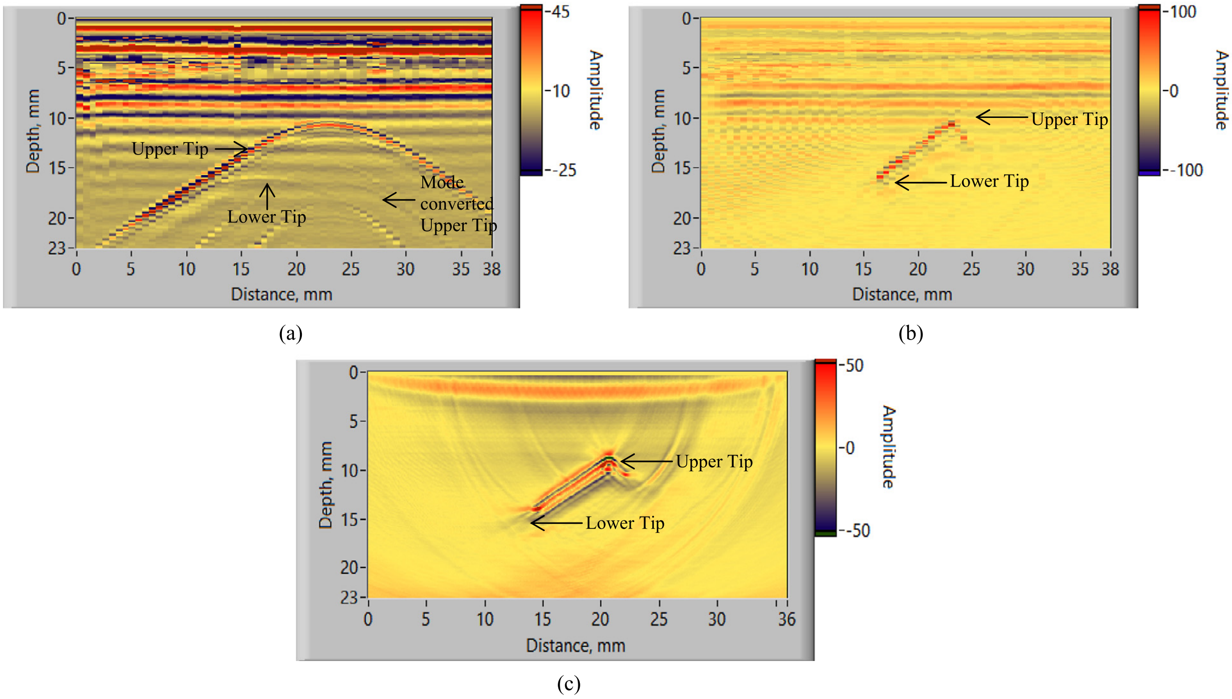


**Fig. 5.** B-scan image for a 51° oriented flaw (a) raw SFLA data, (b) processed SFLA data and (c) FMC + TFM data.

**Table 1**
Results of height and orientation assessment of inclined slots in the stainless steel plate by SFLA and FMC + TFM approaches.

| True angle (deg.) | True depth (mm) | SFLA | | FMC | |
|---|---|---|---|---|---|
| | | Angle (deg.) | Depth (mm) | Angle (deg.) | Depth (mm) |
| 0 | 8.5 | 0 | 8.2 | 0 | 8.2 |
| 16 | 8.2 | 16 | 8.6 | 16 | 8.6 |
| 28 | 7.5 | 29 | 7.9 | 30 | 7.9 |
| 36 | 6.8 | 37 | 6.7 | 35 | 6.8 |
| 42 | 6.3 | 41 | 6.5 | 42 | 6.6 |
| 51 | 5.3 | 52 | 5.2 | 52 | 5.2 |

not seen clearly in the raw data but appear prominently in the processed image. For flaw of lower orientations (16°), the reflected signal from the flaw does not reach the receiving element due to unfavorable angle of incidence as a result of which the flaw surface is not imaged and only the extremities are seen.

Table 1 shows the results of assessment of flaw height and flaw orientation by SFLA and FMC + TFM approaches. The results obtained by SFLA approach are accurate and comparable to the ones obtained by FMC + TFM approach.

### *4.2. Carbon steel plate with embedded weld flaws*

The weld flaws in the form of lack of side wall fusion and root crack were sized by SFLA and FMC approach. The photographs for these flaws are shown in Fig. 6. The raw and processed SFLA B-scan images for lack of sidewall fusion and root crack are shown in Figs. 7 and 8, respectively. For the lack of sidewall fusion, the raw data clearly reveals two hyperbolic indications, corresponding to the upper and the lower tips. These two signals are reduced to two spots on SAFT processing. For the root crack, only the upper tip is visible, since the flaw is open to the surface. In this case too, the well spread out signal from the crack tip is reduced to a spot upon SAFT processing. The results of FMC + TFM for lack of fusion and crack are shown in Figs. 9 and 10 respectively. The flaw tips are effectively located with better signal to noise ratio as compared to SFLA approach.

The results of estimation of height and orientation of these flaws by SFLA and FMC + TFM are summarized in Table 2. The above results indicate that SFLA is very effective for characterization of weld flaws and hence can be used under factory conditions for inspection of welds in various product forms. It also has a very good potential for characterization of service induced cracks in vessels and pipelines. However, there is a need to carry out extensive performance demonstration exercise to achieve the required level of confidence on this approach.

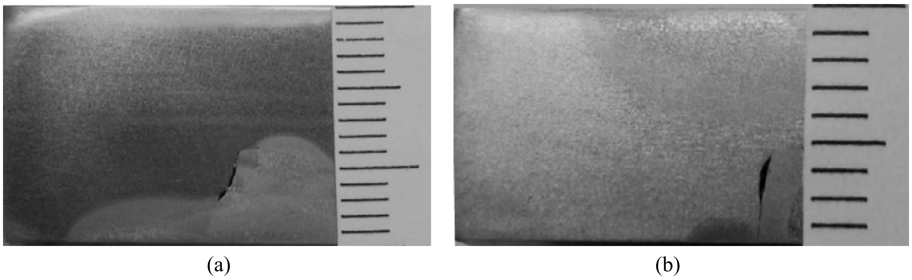

Fig. 6. Photograph of the implanted weld flaws (a) lack of side wall fusion and (b) root crack.

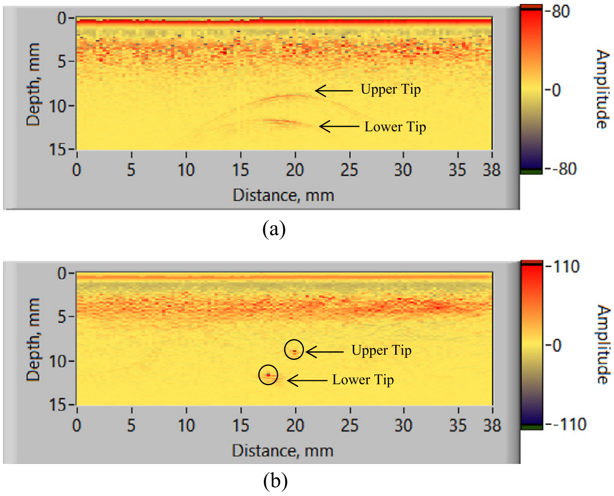


Fig. 7. Raw and processed B-scan images for lack of sidewall fusion using SFLA approach.

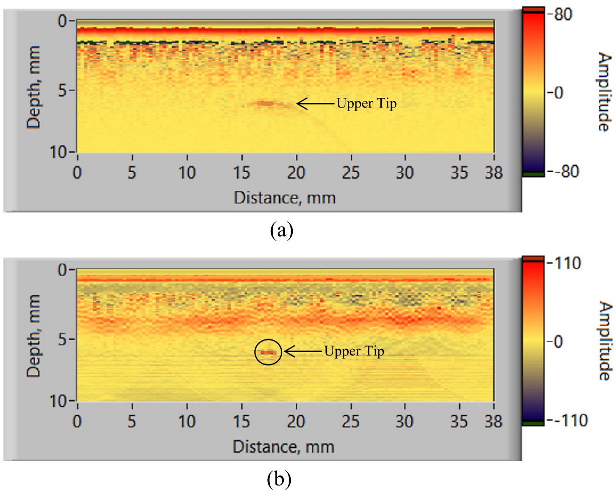


Fig. 8. Raw and processed B-scan images for root crack using SFLA approach.

## 5. Conclusions

Accurate characterization of planar flaws, in terms of orientation and depth, was carried out using an approach combining a linear array and SAFT. The major advantages of this approach are: (i) a single channel instrument with multiplexer is sufficient for data acquisition, (ii) divergent sound beam because of small element size, and small pitch of an array, results in effective SAFT processing and (iii) no computation of focal laws is required, which is a must for conventional phased array. The approach involves SAFT processing of B-scan data collected by divergent sound beam emanating from a single element of a linear array. During this process, the signals from flaw extremities get enhanced and the un-wanted mode converted

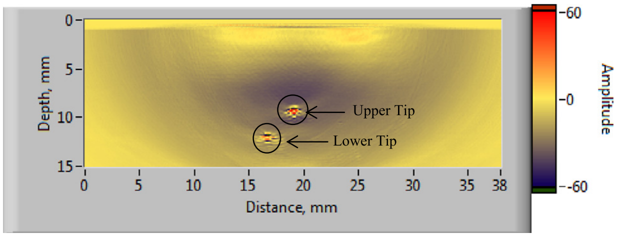


**Fig. 9.** FMC + TFM B-scan image for lack of fusion.

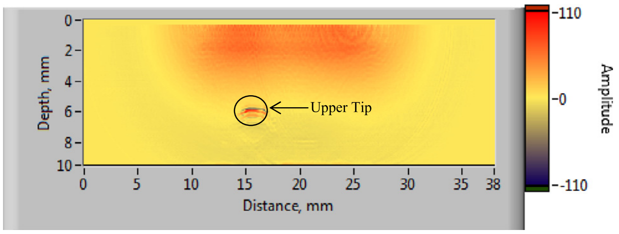


**Fig. 10.** FMC + TFM B-scan image for root crack.

**Table 2**
Assessment of flaw height and orientation in the weld samples by SFLA and FMC + TFM approaches.

| Flaw type | True depth (mm) | True angle (deg.) | SFLA | | FMC | |
|---|---|---|---|---|---|---|
| | | | Angle (deg.) | Depth (mm) | Angle (deg.) | Depth (mm) |
| Lack of fusion | 3.0 | 40 | 39 | 2.9 | 42 | 2.8 |
| Root crack | 3.3 | – | – | 3.5 | – | 3.6 |

signals are eliminated. Moreover, with this approach full-face mapping of flaws, especially those which are oriented at higher angles, is possible. Results obtained using SFLA approach on stainless steel plate with simulated planar flaws and carbon steel plates with real weld planar flaws have shown good accuracy in assessment of flaw orientation and flaw height, which are crucial parameters for fitness-for-service assessment.

## Acknowledgements

The authors would like to acknowledge the help rendered by Ms. N. Jothilakshmi of AFD, BARC in carrying out experiments during the course of this work.

## References

[1] Compilation of NDE effectiveness data. European Commission; March 1999.
[2] Nanekar PP, Mangsulikar MD, Shah BK. Development of NDE techniques for in-service inspection of nuclear power plants. J Nondestruct Test Eval 2007;5:21–8.
[3] Sinclair AN, Fortin J, Shakibi B, Honarvar F, Jastrzebski M, Moles MDC. Enhancement of ultrasonic images for sizing of defects by time-of-flight diffraction. Nondestruct Test Eval Int 2010;43:258–64.
[4] Ravenscroft FA, Newton K, Scruby CB. Diffraction of ultrasound by cracks: comparison of experiment with theory. Ultrasonics 1991;29.
[5] Thomson RN. Transverse and longitudinal resolution of the synthetic aperture focusing technique. Ultrasonics 1984:9–15.
[6] Muller W, Schmitz V, Schafer G. Reconstruction by the synthetic aperture focussing technique (SAFT). Nucl Eng Des 1986;94:393–404.
[7] Schmitz V, Chakhlov S, Muller W. Experiences with synthetic aperture focusing technique in the field. Ultrasonics 2000;38:731–8.
[8] Langenberg KJ, Berger M, Kreutter Th, Mayer K, Schmitz V. Synthetic aperture focusing technique signal processing. Nondestruct Test Eval Int 1986;19:177–89.
[9] Gebhardt W. Improvement of ultrasonic testing by phased arrays. Nucl Eng Des 1983;76:275–83.
[10] Uchida K, Nagaii S, Kashiwaya H, Arii M. Availability study of a phased array ultrasonic technique. Nucl Eng Des 1984;81:309–14.
[11] Portzgen N, Gisolf D, Blacquiere G. Inverse wave field extrapolation: a different NDI approach to imaging defects. IEEE Trans Ultrason Ferroelectr Freq Control 2007;54:118–27.
[12] Holmes C, Drinkwater BW, Wilcox PD. Post-processing of the full matrix of ultrasonic transmit–receive array data for non-destructive evaluation. Nondestruct Test Eval Int 2005;38:701–11.
[13] Lines DIA, Wharrie J, Hottenroth J. Real-time full matrix capture + total focusing and other novel imaging options using general purpose PC-based array instrumentation. Insight 2012;54:86–90.
[14] ASME boiler and pressure vessel code, Section V, Non-destructive methods of examination.